Suplemento de la Revista Mexicana de Física **6** 011302 (2025) 1–7

An information-theoretical take on electron-nuclear wave packet dynamics

Peter Schürger

Institut de Chimie Physique, Université Paris-Saclay.

Received 1 March 2025; accepted 22 March 2025

Applications of information-theoretic measures to a time-dependent coupled electron-nuclear system to analyze the dynamics and correlation between both particles are presented. For this, differential Shannon entropies that are derived from time-dependent coordinate-space and momentum-space probability densities are calculated. Two distinct scenarios are investigated: one exhibiting adiabatic Born-Oppenheimer dynamics and the other involving strong non-adiabatic transitions. The total and single-particle entropies, as well as the mutual information are analyzed and compared to semi-analytical expressions. The results reveal that in the adiabatic regime, correlations manifest differently in coordinate and momentum spaces, which is related to the formation of nodes. In the non-adiabatic case, entropies can be decomposed into state-specific contributions, revealing information about the transition between adiabatic states.

Keywords: Shannon entropy; electron-nuclear dynamics; quantum dynamics; non-adiabatic dynamics.

DOI: https://doi.org/10.31349/SuplRevMexFis.6.011302

1. Introduction

Major advances have been made in recent years in the field of short-time spectroscopy [1], which also brings the many advances in numerical simulations of femtosecond dynamics into the spotlight [2-4]. There, a detailed understanding of the quantum mechanical behavior of all the particles involved, namely, electrons and nuclei, is required. However, their interaction and correlated movement play a crucial role in many aspects of quantum chemistry, underpinning processes ranging from light-induced excitation to charge transfer and bond breaking/forming [5,6]. Further effects and discussions on electron-nuclear correlation can be found in Refs. [7-12].

The equation, that governs the dynamics of electrons and nuclei, is the time-dependent Schrödinger equation,

$$\hat{H}\psi(\mathbf{r},\mathbf{R},t) = i\frac{\partial}{\partial t}\psi(\mathbf{r},\mathbf{R},t), \tag{1}$$

with nuclear coordinates $\mathbf{R}$ and electronic coordinates $\mathbf{r}$. Here, $\hat{H}$ is a molecular Hamiltonian, consisting of the nuclear kinetic energy operator $\hat{T}_{\text{nuc}}$, the electronic kinetic energy operator $\hat{T}_{\text{el}}$, and the potential energy $V(\mathbf{r},\mathbf{R})$. We define the electronic Hamiltonian $\hat{H}_{\text{el}}$ as:

$$\hat{H} = \hat{T}_{\text{nuc}} + \underbrace{\hat{T}_{\text{el}} + V(\mathbf{r},\mathbf{R})}_{\hat{H}_{\text{el}}}. \tag{2}$$

If we fix $\mathbf{R}$ and solve for the eigenstates of $\hat{H}_{\text{el}}$, we find that the states $\varphi_n(\mathbf{r};\mathbf{R})$, that are parametric in $\mathbf{R}$, build an orthonormal basis for the molecular wave function:

$$\Psi(\mathbf{r},\mathbf{R},t) = \sum_n \chi_n(\mathbf{R},t)\varphi_n(\mathbf{r};\mathbf{R}), \tag{3}$$

with nuclear coefficients $\chi_n(\mathbf{R})$. The states $\varphi_n(\mathbf{r};\mathbf{R})$ are referred to as *adiabatic states* of the molecular Hamiltonian. Furthermore, the eigenvalues of $\hat{H}_{\text{el}}$ act as potential energy surfaces for the nuclear degrees of freedom and therefore, are also called *adiabatic potentials*.

Figure 1 illustrates a typical situation based on the example of the Ring=CH_2 stretch mode of fulvene schematically [13]. There, the potential energy surface of the adiabatic ground state and the first excited adiabatic state are presented, as well as with the nuclear density $\rho^{\text{nuc}}(R_{\text{stretch}})$. Initially, $\rho^{\text{nuc}}(R_{\text{stretch}})$ evolves on the excited state potential energy surface. However, when excited state and ground state potential are approaching each other, which is referred to as a conical intersection (or avoided crossing in one dimension), the population can be transferred to the ground state. Therefore, a non-adiabatic transition takes place. Later, the density is reflected and on the second passage of the conical intersection, a less complete population transfer occurs so that both shown states are populated. Due to the high dimensionality of many molecules, replicating the exact dynamics is computationally impossible, and approximate solutions to the time-dependent Schrödinger equation are applied. However, this requires detailed understanding of the wavepacket dynamics and the behavior of densities during the dynamics and, in par-

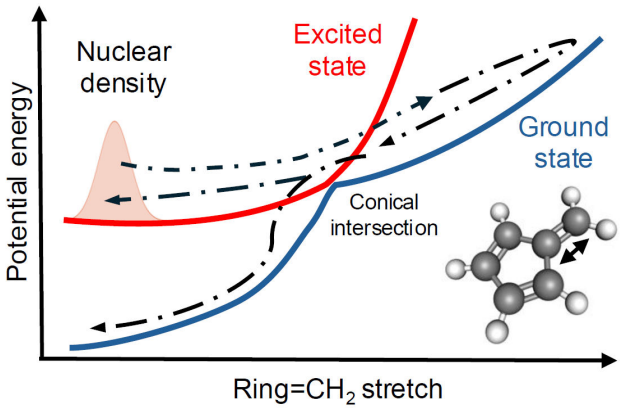

FIGURE 1. Schematic representation of the adiabatic potentials and short-time dynamics of the Ring=CH_2 stretch mode of fulvene.

ticular, the correlated movement of electrons and nuclei. Information-theoretical measures provide a variety of tools to analyze densities and correlations present but their application to dynamical situations is sparse. Here, we will discuss an application of information-theoretical measures.

Another situation of great interest is, when potential energy surfaces are well separated and the dynamics take only place in one electronic state and the Born-Oppenheimer approximation [14] can be applied:

$$\Psi_{BO}(\mathbf{r},\mathbf{R},t) = \chi^{BO}(\mathbf{R},t)\varphi_n(\mathbf{r};\mathbf{R}), \tag{4}$$

where n is the label of the adiabatic potential on which the dynamics take place on. Note, that within this approximation, in the evolution, equations coupling terms to other potential surfaces are neglected. This approximation is fundamental to many applications in quantum chemistry [15].

In the following, we consider both of these situations: first, a situation where the energy surfaces are weakly coupled and well separated, so that the Born-Oppenheimer approximation is expected to hold. Secondly, a situation, where the surfaces are strongly coupled and a nearly complete population transfer takes place. Both situations are analyzed using information theoretical measures, namely, the differential Shannon entropy (DSE) and the mutual information (MI) that are calculated from total and marginal densities obtained from the molecular wave function. Herby, we define the DSE of a density as [16]

$$S[\rho(\mathbf{x})] = \int d\mathbf{x}\, \rho(\mathbf{x}) \ln \rho(\mathbf{x}), \tag{5}$$

where $\mathbf{x}$ is to be replaced by all position (or momentum) variables of the respective density $\rho(\mathbf{x})$ so that we obtain total and single-particle entropies in position and momentum space. We use the MI to measure the non-linear correlation between the electronic and nuclear degrees of freedom. Since we will only encounter one electronic and one nuclear dimension, the MIs in position space and momentum space are defined as

$$I = S[\rho^{el}] + S[\rho^{\text{nuc}}] - S[\rho_{\text{tot}}], \tag{6}$$

$$\tilde{I} = S[\tilde{\rho}^{el}] + S[\tilde{\rho}^{\text{nuc}}] - S[\tilde{\rho}_{\text{tot}}], \tag{7}$$

where the MI I measures non-linear correlations in position space and $\tilde{I}$ in momentum space. In Eq. (6), Eq. (7), we encounter the total position density $\rho(r,R,t) = |\Psi(r,R,t)|^2$, the nuclear position density $\rho^{\text{nuc}}(R,t) = \int dr |\Psi(r,R,t)|^2$ and the electron position density $\rho^{el}(r,t) = \int dR |\Psi(r,R,t)|^2$, as well as the total momentum density $\tilde{\rho}(p,P,t) = |\tilde{\Psi}(p,P,t)|^2$, which is calculated as the absolute square of the Fourier transformation of the molecular wave function. Further, the nuclear momentum density $\tilde{\rho}^{\text{nuc}}(P,t)$ and the electron momentum density $\tilde{\rho}^{\text{nuc}}(p,t)$ are calculated analogously to position space by integrating out the electron momentum p and nuclear momentum P, respectively. Variances, which we will refer to as nuclear/electronic widths, covariances and linear correlation coefficients are calculated from the respective densities as known from statistics [17]. Note that all here defined quantities are time-dependent.

2. Information-theoretical measures applied to coupled electron-nuclear motion

Detailed numerical simulations were carried out using the gird-based split-operator method [18,19] to evolve the molecular wavefunction and analyze the associated densities using information-theoretical measures in a series of papers [20-23]. We will here reference and summarize the results and conclusions presented there. Note that additionally, previous unpublished data is contained in Fig. 5 and 6, namely the propagation within the Born-Oppenheimer approximation, where the same numerical input is utilized as in Ref. [21].

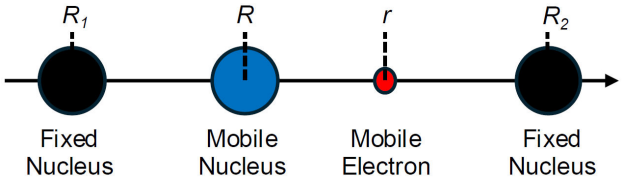

FIGURE 2. The Shin-Metiu model.

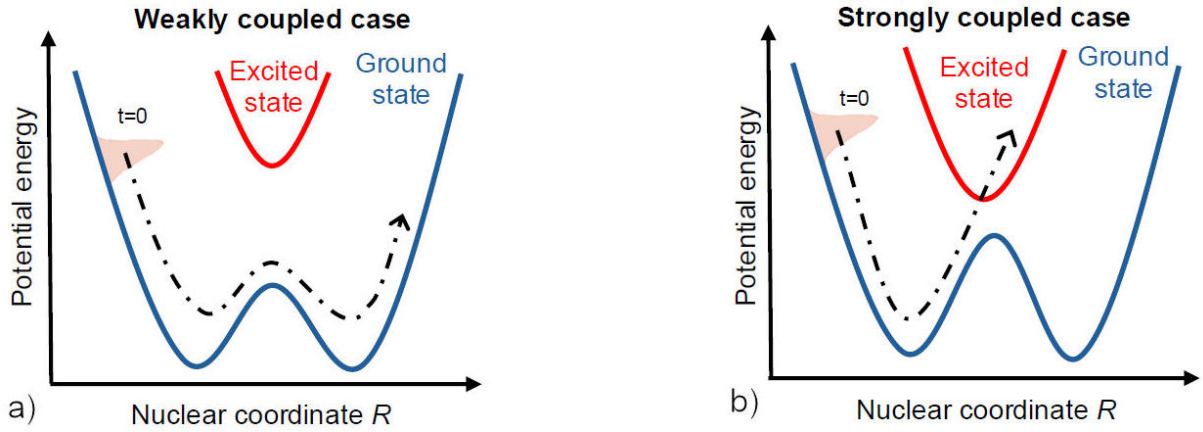

FIGURE 3. Schematic representation of the adiabatic potential energy surfaces and the dynamics for the weakly and strongly coupled cases.

The model applied to study the coupled electron-nuclear motion is the one-dimensional Shin-Metiu model, which was originally introduced to simulate the transfer of an electron and a sodium ion between two zeolite cages [24,25]. However, it proved to be useful as a tool to study non-trivial quantum dynamics by solving the time-dependent Schrödinger equation numerically exact in wide-ranging contexts [8,26-31]. The model consists of two fixed nuclei at positions R_1 and R_2 that interact with a mobile nucleus at R and a mobile electron at r. In explicit, the potential is given as

$$V(r,R) = \frac{1}{|R_1 - R|} + \frac{1}{|R_2 - R|} - \frac{erf[|R_1 - r|/R_f]}{|R_1 - r|} - \frac{erf[|R_2 - r|/R_f]}{|R_2 - r|} - \frac{erf[|R - r|/R_c]}{|R - r|}. \quad (8)$$

The choice of parameters R_f and R_c allows accessing different coupling regimes between electronic and nuclear degrees of freedom. As noted before, we generate a weakly and a strongly coupled case, compare Fig. 3. In both cases, the nuclear degrees of freedom are initialized by an excited Gaussian wavepacket, while the electronic degrees of freedom are prepared in an electronic eigenstate.

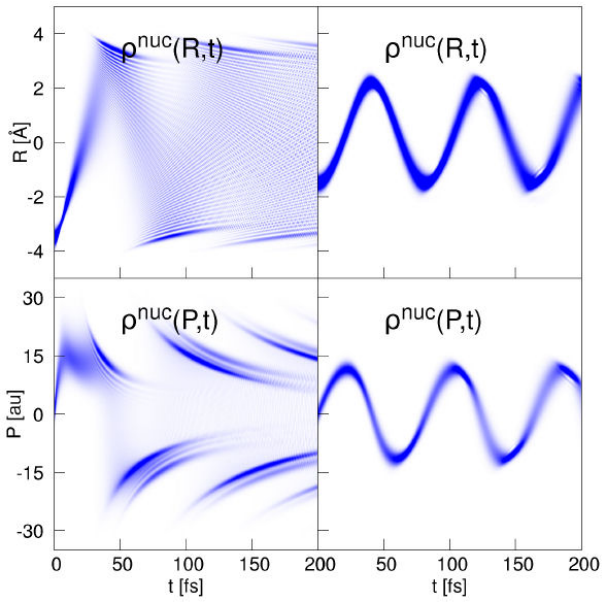

FIGURE 4. Nuclear densities in position and momentum space, for the weakly coupled (left) and strongly coupled (right) cases. Reproduced from Ref. [21].

2.1. Weakly coupled case

Coupling the ground- and exited states only weakly results in a well-defined gap between both states. Then, the nuclear motion happens nearly exclusively on the ground state. The numerical result from the dynamics of the nuclear position density is shown in the top left panel of Fig. 4. There, it can be seen that the initial Gaussian density moves across the system until it is reflected on the opposite potential wall due to the repulsion of the fixed nucleus at R_2. This process repeats periodically while the wave packet disperses. Below that, the dynamics of the nuclear momentum density is shown, where it shows a less coherent dynamics and takes a more complex structure than in position space. The entropies $S_R^{\text{nuc}}(t)$ and $S_P^{\text{nuc}}(t)$ of these two nuclear densities are presented by the red lines labeled "num" in the upper panels of Fig. 5 together with that of the electron densities $S_r^{el}(t)$ and $S_p^{el}(t)$ (middle panels) and total densities $S_X(t)$ and $S_\pi(t)$ (lower panels). Additionally, the blue line indicates the same dynamics but within the Born-Oppenheimer approximation, which are identical to the numerically exact entropies.

Note, that the dynamics of all entropies in the respective spaces are closely related, as minima and maxima are found at similar times. Since in Ref. [20] it was observed that these dynamics are also similar to the dynamics of the widths in position space, (or momentum space, respectively). We formulate the hypothesis that the entropy dynamics are given by a single dynamical variable, the nuclear position (or momentum) width. Therefore, we chose an analytical ansatz for the wavefunction in position space, that reflects in particular the Born-Oppenheimer nature of the dynamics:

$$\Psi(r,R,t) = \underbrace{\left[\frac{\beta_t}{\pi}\right]^{\frac{1}{4}} e^{-\frac{\beta_t}{2}(R-R_t)^2}}_{\text{Nuc. Gaussian Wavepacket}} \times \underbrace{\left[\frac{\gamma}{\pi}\right]^{\frac{1}{4}} e^{-\frac{\gamma}{2}(r-R)^2}}_{\text{El. Eigenfunction}}. \quad (9)$$

Here, the first term represents a Gaussian shaped nuclear wavepacket, which is centered at R_t and has width $1/2\beta_t$. The second term, the electronic eigenfunction, is centered at R and has width $1/2\gamma$, which we assume to be constant. Using this, the analytical expressions for all examined quantities in position space in terms of β_t are calculated. Note that the quantities in momentum space can be calculated using the Fourier transform of Eq. (9). Then, β_t is determined numerically for each time-step using the relation to the nuclear position width for quantities in position space and using the nuclear momentum width for quantities in momentum space. The explicit equations can be found in Refs. [21,22]. The results are the green lines labeled "approx" in Fig. 5. There, we see that the derived approximate expressions indeed reproduce the dynamics of the entropies qualitatively, in both position and momentum space. In particular, the electronic entropies are represented very well, which is not expected since the only dynamical input is related to the nucleus. The differences found in the total and nuclear entropy is due to the fact that for later times the nuclear density structure is more complex than the Gaussian ansatz chosen in Eq. (9).

In Fig. 6 the correlation measures are presented, *i.e.*, the covariance $cov(t)$, the linear correlation coefficient $corr(t)$

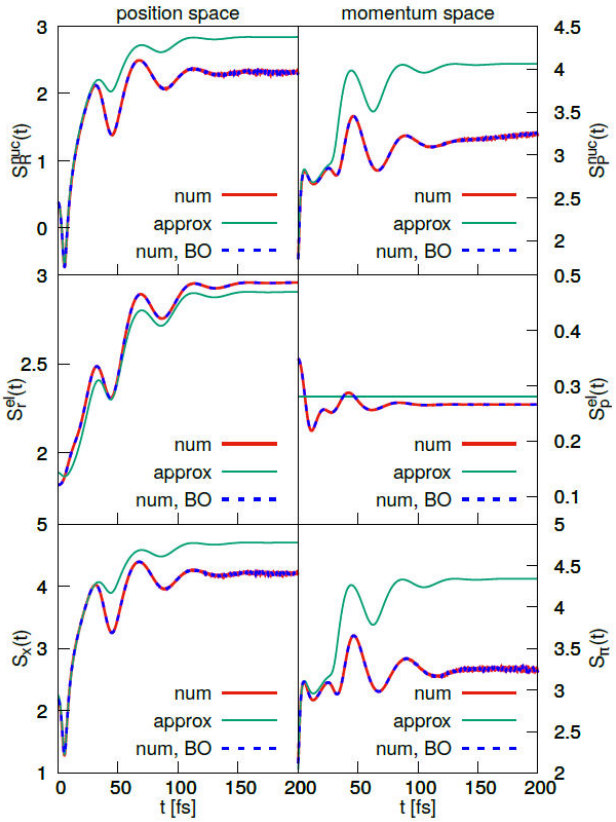

FIGURE 5. Entropy dynamics for the weakly coupled case. This figure contains data published in Ref. [21].

(LCC) and the MI $I(t)$ in both position and momentum space. As previously, the comparison between the numerically exact values, the values calculated within the Born-Oppenheimer approximation and the ones using the derived approximate analytical expressions shows, that they agree very well in position space, indicating that the molecular wavefunction is indeed in Born-Oppenheimer form. In momentum space, however, we encounter larger mismatches: in the linear correlation measures, namely the covariance and the LCC, the values within the BO approximation and the analytically derived ones agree, while they are both distinct from the exact values. Therefore, from a momentum space point of view, the linear correlation within BO approximation is represented worse than in position space. Furthermore, for the MI the numerically exact and the BO values agree very well, while the analytical expression cannot replicate the increase and instead nearly vanishes. This means, that higher-order correlations instead are well represented by the BO-approximation, but an effect arises that is not described by the analytical ansatz in Eq. (9).

We indeed find that the increase of MI is related to the formation of nodes during the dynamics. We showed [23], that the alignment and number of nodes can lead to an increase of the MI of a density. *I.e.*, in position space, the nodes are aligned parallel to the electron coordinate axis so here, the influence of the nodes is negligible. But in momentum space, due to the Fourier relationship, the nodes are diagonally aligned

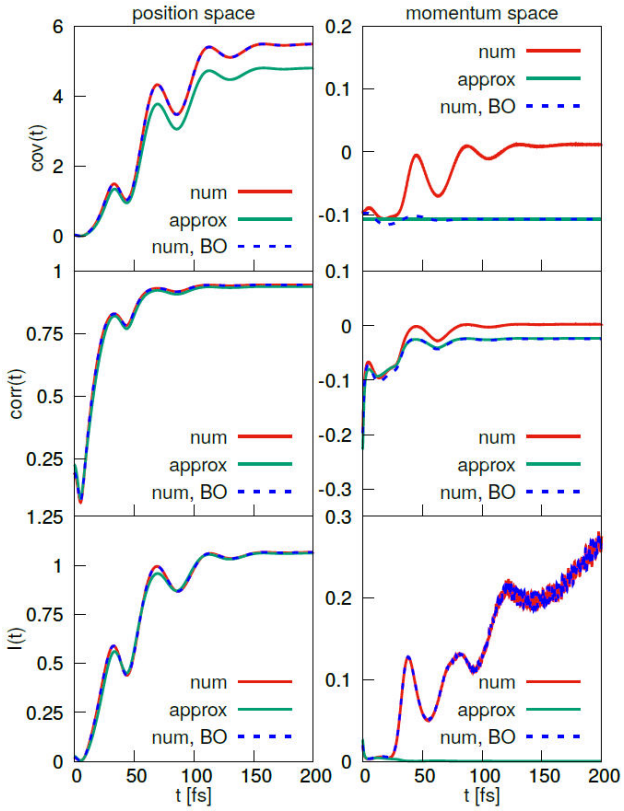

FIGURE 6. Correlation dynamics for the weakly coupled case. This figure contains data published in Ref. [21].

so that they vanish when integrating out one or the other degree of freedom. This then leads to a non-vanishing contribution to the MI. This effect can be included in Eq. (9) by introducing, *e.g.*, excited Harmonic states with a similar number of nodes than observed in the simulation. Then, the increase of the MI can be replicated approximately. In Fig. 6 the correlation measures are presented, *i.e.*, the covariance $cov(t)$, the linear correlation coefficient $corr(t)$ (LCC) and the MI $I(t)$ in both position and momentum space. As previously, the comparison between the numerically exact values, the values calculated within the Born-Oppenheimer approximation and the ones using the derived approximate analytical expressions shows that they agree very well in position space, indicating that the molecular wavefunction is indeed in Born-Oppenheimer form. In momentum space, however, we encounter larger mismatches: in the linear correlation measures, namely the covariance and the LCC, the values within the BO approximation and the analytically derived ones agree, while they are both distinct from the exact values. Therefore, from a momentum space point of view, the linear correlation within BO approximation is represented worse than in position space. Furthermore, for the MI the numerically exact and the BO values agree very well, while the analytical expression cannot replicate the increase and instead nearly vanishes. This means that higher-order correlations instead are well represented by the BO-approximation, but an

effect arises that is not described by the analytical ansatz in Eq. (9). We find that the increase of MI is related to the formation of nodes during the dynamics. We showed [23], that the alignment and number of nodes can lead to an increase of the MI of a density. *I.e.*, in position space, the nodes are aligned parallel to the electron coordinate axis so here, the influence of the nodes is negligible. But in momentum space, due to the Fourier relationship, the nodes are diagonally aligned so that they vanish when integrating out one or the other degree of freedom. This then leads to a non-vanishing contribution to the MI. This effect can be included in Eq. (9) by introducing, *e.g.*, excited Harmonic states with a similar number of nodes as observed in the simulation. Then, the increase of the MI can be replicated approximately.

2.2. Strongly coupled Case

In the strongly coupled case, the avoided crossing allows for nearly complete population transfer between the ground- and excited state, as indicated in the lower panel of Fig. 3. The dynamics of the nuclear position density is presented in the upper right panel of Fig. 4 and yields nearly harmonic oscillations with only very weak dispersion visible. The nuclear momentum density (lower bottom panel of Fig. 4) shows similar behavior, with the typical phase shift compared to the position space, known from the harmonic oscillator. Note that during the considered time frame, the electron remains bound to one of the fixed nuclei of the Shin-Metiu model and shows no dynamics. The entropy dynamics were studied in detail in Ref. [20]. There, we find that the nuclear entropy oscillates similar to the nuclear width, while electronic quantities remain basically constant. Further, we see that the total entropy is approximately the sum of the electronic and nuclear entropy, resulting in the MI to vanish. Therefore, in the considered setup, only negligible correlations are present. In a similar approach to the weakly coupled case, we chose an analytic ansatz to relate the entropy dynamics to the nuclear widths:

$$\Psi(r,R,t) = \underbrace{\left[\frac{\beta_t}{\pi}\right]^{\frac{1}{4}} e^{-\frac{\beta_t}{2}(R-R_t)^2}}_{\text{Nuc. Gaussian Wavepacket}} \times \underbrace{\left[\frac{\gamma}{\pi}\right]^{\frac{1}{4}} e^{-\frac{\gamma}{2}(r-R_0)^2}}_{\text{El. Eigenfunction}}, \quad (10)$$

where β_t is determined from nuclear position width, or momentum width, respectively, and γ is chosen constant. Note that in contrast to Eq. (9), the electronic eigenfunction centered at a fixed nuclear position R_0, reflecting the observed dynamics. We find that the quantities calculated from this ansatz yield excellent agreement with analytic properties in position and momentum space [21], indicating that here, the density dynamics are purely described by the nuclear width. Eq. (10) also illustrates that the total density, therefore the absolute square of Eq. (10), is of an uncorrelated product form. This results in vanishing linear correlation measures as well as in the vanishing MI.

Since multiple electronic states are involved in the strongly coupled case, it is interesting to consider the decomposition of the total density

$$\rho(r,R,t) = \sum_{n,m} \rho_{nm}(r,R,t) = \sum_{n,m} \chi_n(R,t)\chi_m^*(R,t)\varphi_n(r;R)\varphi_m^*(r;R), \quad (11)$$

derived from the Born-Huang expansion Eq. (3). Note, that diagonal terms of the density decomposition are real and positive semi-definite and therefore, we define decomposed entropies, *e.g.*,

$$S_X^n(t) = \int dr dR\, \rho_{nn}(r,R,t) \ln \rho_{nn}(r,R,t). \quad (12)$$

Similar definitions can be obtained for the electronic and nuclear entropies. Note, that then, the sum over the respective decomposed entropies, *e.g.*, $\sum_n S_X^n(t)$ behaves as a DSE as well, while the individual decomposed entropies carry information about the population of the states, that leads to warped transformation behavior under coordinate transformations, see [32] for a detailed discussion. The entropy sums can be compared to their not-decomposed counterparts, *e.g.*, $\sum_n S_X^n(t)$ and $S_X(t)$. Interestingly, we find that in position space, the total entropy and the nuclear entropy are equivalent to the decomposed entropy sums, but the decomposed electronic entropy sum shows spikes at non-adiabatic transitions. This is related to details of the transition for the respective density. If there is no density overlap present, we observe no spikes as for the nucleus and if there is significant overlap, as is for the electron, we observe spikes that were shown to be related to the population transfer. A deeper study on decomposed entropies was conducted in Ref. [33] on a similar system.

3. Conclusion

We presented a non-standard approach to quantum dynamics, revealing a new perspective on coupled electron-nuclear motion by using information-theoretical measures calculated from time-dependent densities of the considered system. We showed how differential Shannon entropy can be used to analyze the dynamics and how mutual information can be applied to study the correlation between the particles. In detail, we presented two case studies. One, where the potential energy surfaces are weakly coupled, so that the Born-Oppenheimer approximation can be studied, and one that involves strong coupling to study how densities behave under population transfer. In the first, we show that while the Born-Oppenheimer successfully replicates correlations in position space, correlations in momentum space are not. Further, we argue that nodal structure is relevant to understand the mutual information in momentum space. In the second, strongly

coupled case, the dynamics are simpler and correlations vanish. However, by defining decomposed entropies, we gain information on the details of non-adiabatic transitions between electronic states. Finally, we note that exploring an "intermediate" coupling regime would be intriguing; however, this will be addressed in future work.

Acknowledgements

The author would like to express his deepest gratitude to his former supervisor, Prof. Volker Engel, for his invaluable guidance, support, and encouragement throughout the course of this research.

1. D. Rolles, Time-resolved experiments on gas-phase atoms and molecules with XUV and X-ray free-electron lasers, *Advances in Physics: X* **8** (2023) 2132182. https://doi.org/10.1080/23746149.2022.2132182
2. J. P. Figueira Nunes *et al*., Monitoring the Evolution of Relative Product Populations at Early Times during a Photochemical Reaction, *J. Am. Chem. Soc.* **146** (2024) 4134. https://doi.org/10.1021/jacs.3c13046
3. S. Pathak *et al*., Tracking the ultraviolet-induced photochemistry of thiophenone during and after ultrafast ring opening, *Nature Chem.* **12** (2020) 795. https://doi.org/10.1038/s41557-020-0507-3
4. S. B. Muvva *et al*., Ultrafast structural dynamics of UV photoexcited cis,cis-1,3-cyclooctadiene observed with timeresolved electron diffraction, *Phys. Chem. Chem. Phys.* (2024). https://dx.doi.org/10.1039/D4CP02785J
5. D. J. Tannor, Introduction to Quantum Mechanics - a Time-Dependent Perspective (University Science Books, Sausalito, California, 2007).
6. L. González and R. Lindh, Quantum Chemistry and Dynamics of Excited States: Methods and Applications (JohnWiley & Sons, Chichester, 2020). https://doi.org/10.1002/9781119417774
7. E. A. Arsenault *et al.*, Vibronic coupling in energy transfer dynamics and two-dimensional electronic-vibrational spectra, *J. Chem. Phys.* **155** (2021) 054201, https://doi.org/10.1063/5.0056477.
8. K. M. Ziems *et al*., Nuclear-Electron Correlation Effects and Their Photoelectron Imprint in Molecular XUV Ionisation, *Front. Chem.* **10** (2022) 942633, https://doi.org/10.3389/fchem.2022.942633.
9. M. V. Pak and S. Hammes-Schiffer, Electron-Proton Correlation for Hydrogen Tunneling Systems, *Phys. Rev. Lett.* **92** (2004) 103002, https://doi.org/10.1103/physrevlett.92.103002.
10. S. A. González and A. Reyes, Nuclear quantum effects on the He2H+ complex with the nuclear molecular orbital approach, *Int. J. Quantum Chem.* **110** (2009) 689, https://doi.org/10.1002/qua.22118.
11. F. Agostini, E. Gross, and B. F. Curchod, Electron-nuclear entanglement in the time-dependent molecular wavefunction, *Comput. Theor. Chem.* **1151** (2019) 99, https://doi.org/10.1016/j.comptc.2019.01.021.
12. J. Stetzler and V. A. Rassolov, Comparison of Born-Oppenheimer approximation and electron-nuclear correlation, *Mol. Phys.* **121** (2022) e2106321, https://doi.org/10.1080/00268976.2022.2106321.
13. P. Schürger *et al.*, Assessing the performance of coupledtrajectory schemes on full-dimensional two-state linear vibronic coupling models, *J. Chem. Phys.* **162** (2025) 104117, https://doi.org/10.1063/5.0252505.
14. M. Born and R. Oppenheimer, Zur Quantentheorie der Molekeln, *Ann. Phys.* **389** (1927) 457, https://doi.org/10.1002/andp.19273892002.
15. A. Szabo and N. S. Ostlund, Modern quantum chemistry, Dover Books on Chemistry (Dover Publications, Mineola, NY, 1996).
16. J. V. Michalowicz, J. M. Nichols, and F. Bucholtz, Handbook of differential entropy (Chapman & Hall/CRC, Philadelphia, PA, 2018).
17. C.W. Gardiner, Handbook of Stochastic Methods - For Physics, Chemistry and the Natural Sciences 2nd ed. (Springer-Verlag, Berlin, Heidelberg, 1985).
18. M. Feit, J. Fleck, and A. Steiger, Solution of the Schrödinger equation by a spectral method, *J. Comput. Phys.* **47** (1982) 412, https://doi.org/10.1016/0021-9991(82)90091-2.
19. M. D. Feit and J. A. Fleck, Solution of the Schrödinger equation by a spectral method II: Vibrational energy levels of triatomic molecules, *J. Chem. Phys.* **78** (1983) 301, https://doi.org/10.1063/1.444501.
20. P. Schürger and V. Engel, Information Theoretical Approach to Coupled Electron-Nuclear Wave Packet Dynamics: Time-Dependent Differential Shannon Entropies, *J. Phys. Chem. Lett.* **14** (2023) 334, https://doi.org/10.1021/acs.jpclett.2c03635.
21. P. Schürger and V. Engel, Differential Shannon Entropies Characterizing Electron-Nuclear Dynamics and Correlation: Momentum-Space Versus Coordinate-Space Wave Packet Motion, *Entropy* **25** (2023) 970, https://doi.org/10.3390/e25070970.
22. P. Schürger and V. Engel, Differential Shannon entropies and correlation measures for Born-Oppenheimer electron-nuclear dynamics: numerical results and their analytical interpretation, *Phys. Chem. Chem. Phys.* **25** (2023) 28373, https://doi.org/10.1039/D3CP03573E.
23. P. Schürger and V. Engel, On the relation between nodal structures in quantum wave functions and particle correlation, *AIP Advances* **13** (2023) 125307, https://doi.org/10.1063/5.0180004.
24. S. Shin and H. Metiu, Nonadiabatic effects on the charge transfer rate constant: A numerical study of a simple model system, *J. Chem. Phys.* **102** (1995) 9285, https://doi.org/10.1063/1.468795.

25. S. Shin and H. Metiu, Multiple Time Scale Quantum Wavepacket Propagation: Electron-Nuclear Dynamics, *J. Phys. Chem.* **100** (1996) 7867, https://doi.org/10.1021/jp952498a.

26. M. Erdmann, P. Marquetand, and V. Engel, Combined electronic and nuclear dynamics in a simple model system, *J. Chem. Phys.* **119** (2003) 672, https://doi.org/10.1063/1.1578618.

27. M. Falge, V. Engel, and S. Gräfe, Time-resolved photoelectron spectroscopy of coupled electron-nuclear motion, *J. Chem. Phys.* **134** (2011) 184307, https://doi.org/10.1063/1.3585692.

28. M. Falge, V. Engel, and S. Gräfe, Fingerprints of Adiabatic versus Diabatic Vibronic Dynamics in the Asymmetry of Photoelectron Momentum Distributions, *J. Phys. Chem. Lett.* **3** (2012) 2617, https://doi.org/10.1021/jz3009826.

29. J. Albert *et al.*, Communication: Vibrational and vibronic coherences in the two dimensional spectroscopy of coupled electron-nuclear motion, *J. Chem. Phys.* **143** (2015) 041102, https://doi.org/10.1063/1.4927396.

30. F. G. Fröbel *et al.*, The impact of electron-electron correlation in ultrafast attosecond single ionization dynamics, *J. Phys. B: At. Mol. Opt. Phys.* **53** (2020) 144005, https://doi.org/10.1088/1361-6455/ab8c21.

31. T. Schaupp and V. Engel, BornOppenheimer contributions to time-dependent electron momenta, *J. Chem. Phys.* **152** (2020) 204310, https://doi.org/10.1063/5.0004560.

32. P. Schürger, Information-Theoretical Studies on Time- Dependent Quantum Systems, doctoralthesis, Universität Würzburg (2024), https://doi.org/10.25972/OPUS-35221.

33. P. Schürger and V. Engel, Differential Shannon Entropies and Mutual Information in a Curve Crossing System: Adiabatic and Diabatic Decompositions, *J. Chem. Theory Comput.* **20** (2024) 5012, https://doi.org/10.1021/acs.jctc.4c00245.